


METHODOLOGY ARTICLE

Open Access



Streamlined alpha-synuclein RT-QuIC assay for various biospecimens in Parkinson's disease and dementia with Lewy bodies

Connor Bargar¹, Wen Wang¹, Steven A. Gunzler², Alexandra LeFevre³, Zerui Wang¹, Alan J. Lerner², Neena Singh^{1,2}, Curtis Tatsuoka², Brian Appleby^{1,2}, Xiongwei Zhu^{1,2}, Rong Xu⁴, Vahram Haroutunian⁵, Wen-Quan Zou^{1,2*}, Jiyan Ma^{6*} and Shu G. Chen^{1,2*} 

Abstract

Definitive diagnosis of Parkinson's disease (PD) and dementia with Lewy bodies (DLB) relies on postmortem finding of disease-associated alpha-synuclein (αSyn^D) as misfolded protein aggregates in the central nervous system (CNS). The recent development of the real-time quaking induced conversion (RT-QuIC) assay for ultrasensitive detection of αSyn^D aggregates has revitalized the diagnostic values of clinically accessible biospecimens, including cerebrospinal fluid (CSF) and peripheral tissues. However, the current αSyn RT-QuIC assay platforms vary widely and are thus challenging to implement and standardize the measurements of αSyn^D across a wide range of biospecimens and in different laboratories. We have streamlined αSyn RT-QuIC assay based on a second generation assay platform that was assembled entirely with commercial reagents. The streamlined RT-QuIC method consisted of a simplified protocol requiring minimal hands-on time, and allowing for a uniform analysis of αSyn^D in different types of biospecimens from PD and DLB. Ultrasensitive and specific RT-QuIC detection of αSyn^D aggregates was achieved in million-fold diluted brain homogenates and in nanoliters of CSF from PD and DLB cases but not from controls. Comparative analysis revealed higher seeding activity of αSyn^D in DLB than PD in both brain homogenates and CSF. Our assay was further validated with CSF samples of 214 neuropathologically confirmed cases from tissue repositories (88 PD, 58 DLB, and 68 controls), yielding a sensitivity of 98% and a specificity of 100%. Finally, a single RT-QuIC assay protocol was employed uniformly to detect seeding activity of αSyn^D in PD samples across different types of tissues including the brain, skin, salivary gland, and colon. We anticipate that our streamlined protocol will enable interested laboratories to easily and rapidly implement the αSyn RT-QuIC assay for various clinical specimens from PD and DLB. The utilization of commercial products for all assay components will improve the robustness and standardization of the RT-QuIC assay for diagnostic applications across different sites. Due to ultralow sample consumption, the ultrasensitive RT-QuIC assay will facilitate efficient use and sharing of scarce resources of biospecimens. Our streamlined RT-QuIC assay is suitable to track the distribution of αSyn^D in CNS and peripheral tissues of affected patients. The ongoing evaluation of RT-QuIC assay of αSyn^D as a potential biomarker for PD and DLB in clinically accessible biospecimens has broad implications

*Correspondence: wxz6@case.edu; Jiyanma333@gmail.com; shu.chen@case.edu

¹ Department of Pathology, Case Western Reserve University School of Medicine, Cleveland, OH 44106, USA

⁶ Van Andel Institute, Grand Rapids, MI 49503, USA

Full list of author information is available at the end of the article



© The Author(s) 2021. **Open Access** This article is licensed under a Creative Commons Attribution 4.0 International License, which permits use, sharing, adaptation, distribution and reproduction in any medium or format, as long as you give appropriate credit to the original author(s) and the source, provide a link to the Creative Commons licence, and indicate if changes were made. The images or other third party material in this article are included in the article's Creative Commons licence, unless indicated otherwise in a credit line to the material. If material is not included in the article's Creative Commons licence and your intended use is not permitted by statutory regulation or exceeds the permitted use, you will need to obtain permission directly from the copyright holder. To view a copy of this licence, visit <http://creativecommons.org/licenses/by/4.0/>. The Creative Commons Public Domain Dedication waiver (<http://creativecommons.org/publicdomain/zero/1.0/>) applies to the data made available in this article, unless otherwise stated in a credit line to the data.

for understanding disease pathogenesis, improving early and differential diagnosis, and monitoring therapeutic efficacies in clinical trials.

Keywords: Alpha-synuclein, Biomarker, Biospecimens, Cerebrospinal fluid, Colon, Dementia with Lewy bodies, Parkinson's disease, RT-QuIC, Salivary gland, Skin

Introduction

An unmet clinical need is a reliable premortem diagnostic biomarker for Parkinson's disease (PD) and dementia with Lewy bodies (DLB), two common synucleinopathies [1]. Currently, definitive diagnosis of PD and DLB relies mainly on postmortem detection of disease-associated alpha-synuclein ($\alpha\text{Syn}^{\text{D}}$), deposited as protein aggregates within the Lewy body inclusions in the central nervous system (CNS) [2, 3]. Overwhelming evidence suggests that $\alpha\text{Syn}^{\text{D}}$ aggregates are formed as a consequence of protein misfolding cascades and may spread through prion-like transmission across cells and tissues during disease pathogenesis [4]. These $\alpha\text{Syn}^{\text{D}}$ aggregates may potentially serve as a promising biomarker of PD and DLB for premortem diagnosis and treatment. However, detection of $\alpha\text{Syn}^{\text{D}}$ aggregates in easily accessible specimens has been difficult and a clinically validated assay platform remains to be established. Previously, immunoassays have been used to measure various forms of αSyn (total and phosphorylated) in cerebrospinal fluid (CSF), a CNS-derived body fluid. However, the conventional immunoassays of CSF in PD and DLB have thus far yielded inconsistent and disappointing performance for diagnostic purpose [5–7]. Similarly, immunohistochemical (IHC) staining of phosphorylated αSyn has been observed in peripheral tissues of PD and DLB, but wide variations in analytic performance have been reported by various groups as standardization of IHC staining remains a formidable challenge [8–12].

The real-time quaking induced conversion (RT-QuIC) assay has recently emerged as a powerful platform for amplified detection of $\alpha\text{Syn}^{\text{D}}$ aggregates [13]. The αSyn RT-QuIC assay monitors the template-seeded aggregation of recombinant monomeric αSyn into amyloid fibrils upon seeding by traces of $\alpha\text{Syn}^{\text{D}}$ aggregates present in biospecimens. The newly generated β -sheet rich amyloid fibrils bind to an amyloid-sensitive dye, thioflavin T (ThT), resulting an enhanced fluorescence. Recent studies have utilized αSyn RT-QuIC assay to detect seeding activity of $\alpha\text{Syn}^{\text{D}}$ aggregates in brain homogenate (BH) and CSF samples from PD and DLB, with a diagnostic sensitivity great than 90% and specificity of 82–100% for CSF samples [14–17]. Moreover, the αSyn RT-QuIC method has been extended to evaluate the presence of $\alpha\text{Syn}^{\text{D}}$ from non-CNS sources, such as nasal brushing [18], salivary gland [19] and skin [20, 21]. The RT-QuIC

platform has the advantage of high throughput, fast turn-around, and automated recording of aggregation kinetics in real time. However, the published assay conditions for αSyn RT-QuIC vary in both configuration and the sources and compositions of reagents, thus discouraging a broad use of this novel technology in clinical research and disease diagnosis. For example, recombinant αSyn (rec-Syn), the RT-QuIC substrate, was often purified in-house from the expression in *E. coli*, either as the wild-type rec-Syn or an engineered mutant (rec-Syn-K23Q) [15]. This approach demands a considerable technical expertise and a lengthy hands-on time of ~5–7 days. A suitable commercial source of rec-Syn will greatly simplify the implementation of αSyn RT-QuIC assay in a routine laboratory. Moreover, existing RT-QuIC protocols also vary depending on the types of tissue specimens such as brain, CSF, salivary gland, and skin [15, 19–22]. However, it has been unclear whether different assay conditions are indeed required for different tissue matrices. Conceivably, a streamlined RT-QuIC protocol suitable for the detection of $\alpha\text{Syn}^{\text{D}}$ in a diverse array of biospecimens will facilitate the standardized assessment of clinically accessible tissues for the diagnosis of PD and DLB.

In the present study, we have developed a streamlined αSyn RT-QuIC assay through the optimized use of entirely commercial reagents, enabling rapid assembly of assay components with minimal hands-on time. We have validated this streamlined αSyn RT-QuIC assay using a large collection of CSF from neuropathologically confirmed cases of PD, DLB, and non-synucleinopathy (NS) controls, yielding high analytical performance in terms of sensitivity and specificity. Moreover, we have shown that a single RT-QuIC protocol is feasible for ultrasensitive and rapid assay of $\alpha\text{Syn}^{\text{D}}$ in PD across different types of tissues including the brain, skin, salivary gland, and colon.

Methods

Human specimens

All human samples were received as de-identified post-mortem cases originated from the respective sites and collected under the guidelines of local ethics committees. Unless otherwise specified, frozen brain tissue and CSF samples for the development of αSyn RT-QuIC assay were obtained from the NIH NeuroBioBank (NBB), a centralized network of biorepositories. Brain

tissue samples included 3 cases each of PD and DLB with confirmed neuropathology and 3 cases of NS controls archived at NBB. A collection of 214 CSF samples from NBB included cases of PD (n=88), DLB (n=58) and NS controls (n=68) including those from the neurologically normal (n=23), amyotrophic lateral sclerosis (ALS, n=9), multiple sclerosis (MS, n=6), Alzheimer's disease (AD, n=7), Pick's disease (n=10), corticobasal degeneration (CBD, n=4), and progressive supranuclear palsy (PSP, n=9). The demographic data of CSF cases examined for diagnostic validation by RT-QuIC analyses are listed in Table 1. Multiple tissue panels available from the same cadavers included a case of neuropathologically confirmed PD (case number 6164) and a NS control affected by AD (case number 5687) with samples of the brain, scalp skin, and CSF obtained from NBB (used for Fig. 4a), a case of neuropathologically confirmed PD (case number 2054) and a NS control without any neurological disease (case number 2074) with samples of scalp skin, submandibular gland (SMG), sigmoid colon, and CSF obtained from the Banner Sun Health Research Institute (BSHRI, Sun City, Arizona, USA) (used for Fig. 4b), and a case of neuropathologically confirmed PD (case number 2052) and a NS control without any neurological disease (case number 2078) with samples of scalp skin, SMG, sigmoid colon obtained from BSHRI (used for Fig. 5).

Preparation of human specimens

All human biospecimens were received on dry ice and were stored at -80 °C before sample preparation. Frozen brain samples were lysed in ice-cold lysis buffer [Dulbecco's phosphate-buffered saline (PBS) supplemented with 1% Triton X-100, 150 mM NaCl, 5 mM EDTA, and Roche mini-cOmplete™ proteinase inhibitors (Roche Diagnostics, Indianapolis, IN, USA)], followed by homogenization in the presence of zirconia beads (1 mm) in a mini-Beadbeater-16 device

(BioSpec Products, Bartlesville, OK, USA) for 5 cycles of 1 min beating and 3 min cooling at 4 °C. Following a brief centrifugation for 5 min at 500 × g, a 10% brain homogenate (w/v) was prepared and stored at -80 °C until use. For all peripheral tissues, previous studies included a 4-h enzymatic digestion step during tissue extraction [20, 23]. This step was eliminated in our protocol without noticeable changes in extraction efficiency. Frozen samples of scalp skin were thawed, and washed in ice-cold PBS at least three times until no visible blood remained. The skin tissue was minced with a razor blade, followed by homogenization in lysis buffer in the presence of zirconia beads as above. A 10% skin homogenate (w/v) was prepared and stored at -80 °C until use. Frozen samples of SMG and sigmoid colon were prepared in the same manner as the skin, as described above. A 10% homogenate (w/v) of SMG or colon was prepared and stored at -80 °C until use. Frozen samples of CSF were thawed and used immediately before assay without further processing.

Reagents for RT-QuIC assay

All reagents used for αSyn RT-QuIC assay were obtained from commercial sources. Sodium phosphate (0.5 M, pH 8.0) was from Boston BioProducts (Ashland, MA, USA), sodium chloride (5 M) was from Invitrogen (Carlsbad, CA, USA), thioflavin T (ThT) was from Sigma (St. Louis, MO, USA). HPLC-grade water from Thermo Fisher (Waltham, MA, USA) was used to prepare solutions. Aliquots of individual stock solutions were stored at -20 °C until use. Lyophilized recombinant human αSyn (rec-Syn) were purchased from rPeptide (Watkinsville, GA, USA) with catalog number S-1001-02 and lot numbers 082517AS (lot 1) and 111317AS (lot 2), and stored at -20 °C until use.

Table 1 Demographic information for CSF cases and results of αSyn RT-QuIC assay

	PD	DLB	NS Controls							
			Total	Normal	ALS	MS	AD	Picks	CBD	PSP
No	88	58	68	23	9	6	7	10	4	9
Age, years (SD)	78.3 (8.1)	77.2 (8.8)	74.3 (10.9)	79.6(8.3)	72.2 (9.6)	66.3 (9.0)	70.9 (16.7)	68.5 (10.7)	74.5 (4.2)	79.1 (10.1)
Male, no. (%)	58 (66)	37 (64)	36 (53)	14 (61)	3 (33)	0 (0)	3 (43)	10 (100)	3 (75)	3 (33)
RT-QuIC assay										
ThT at 60 h, % (SE)	54.5 (2.2)	64.0 (2.5)	5.2 (0.2)	5.8 (0.4)	5.5 (0.4)	5.5 (0.4)	3.8 (0.4)	4.3 (0.5)	4.4 (0.8)	6.2 (1.6)
<i>P</i> value (compared to PD) ^a	NA	<0.05	<0.0001	<0.0001	<0.0001	<0.0001	<0.0001	<0.0001	<0.0001	0.0003
<i>P</i> value (compared to NS total controls) ^a	<0.0001	<0.0001	NA	>0.99	>0.99	>0.99	>0.99	>0.99	>0.99	>0.99

NA, not applicable

^a *P* values determined by one way analysis of variance with Tukey's post hoc test

RT-QuIC assay procedure and data analysis

For tissue samples, an initial tissue homogenate [10% (w/v), defined as 10^{-1} dilution] as prepared above was subjected to serial tenfold dilutions with sample diluent containing PBS supplemented with Gibco $1 \times N2$ supplement (Thermo Fisher, Waltham, MA, USA). RT-QuIC reactions were performed in Nunc black 96-well plates with optical flat bottom (Thermo Fisher, Waltham, MA, USA). Each well was preloaded with six 0.8 mm low-binding silica beads (OPS Diagnostics, Lebanon, NJ, USA). Lyophilized rec-Syn (rPeptide) was reconstituted in HPLC-grade water to 1 mg/ml and filtered through Amicon 100 kDa filters (Millipore, Burlington, MA, USA) by centrifugation for 10 min at 4 °C. To measure α Syn RT-QuIC seeding activity, 2 μ l of diluted tissue homogenate was added to individual wells containing 98 μ l of RT-QuIC reaction mixture composed of 40 mM NaPO₄ (pH 8.0), 170 mM NaCl, 20 μ M ThT, 0.1 mg/ml rec-Syn. The plates were sealed with Nunc clear sealing film (Thermo Fisher, Waltham, MA, USA) and incubated at 42 °C in a BMG FLUOstar Omega plate reader (BMG Labtech, Cary, NC, USA) with cycles of 1 min shaking (400 rpm, double orbital) and 1 min rest throughout the assay. ThT fluorescence (450 nm excitation and 480 nm emission; bottom read) was recorded every 45 min for 60 h. For CSF samples, 2 μ l of neat CSF or CSF serially diluted with sample diluent was added to individual wells containing 98 μ l of RT-QuIC reaction mixture supplemented with 0.0005% SDS. Four replicate reactions were made for each sample. The plate reader was set up with optic gain setting (~1900) that would give a negative control baseline of ThT fluorescence around 15,000 relative fluorescence units (rfu). The maximal fluorescence response of the plate reader was fixed at 260,000 rfu. Raw data with ThT fluorescence intensity in rfu were normalized to a percentage of the maximal fluorescence at 260,000 rfu (defined as 100%). Positive RT-QuIC reactivity of individual wells is defined as enhanced ThT fluorescence above a predefined threshold within 60 h. This threshold was calculated as the average background fluorescence plus 5 standard deviations, equal to ~30,000 rfu or ~11% of maximum ThT response in our experiments. For RT-QuIC analyses, data from four technical replicates were examined for a given biospecimen. A biospecimen was considered positive when at least two out of the four replicates displayed positive ThT reactivity above the threshold. For each positive sample, the average fluorescence intensity from the positive replicates was calculated and plotted against time. For each negative sample, the average fluorescence intensity from the negative replicates was calculated and plotted against time. The lag phase of RT-QuIC reactions was defined as the time (h) to reach the threshold as defined above. Protein aggregation rate

(PAR) was calculated as the inverse of lag-phase (1/h). For Spearman-Kärber analyses of end-point dilution RT-QuIC experiments, tenfold serial dilutions of a biospecimen were prepared. Each diluted sample was used to seed RT-QuIC reactions in quadruplicate. ThT fluorescence from individual replicates for each dilution were plotted against time. The dilution series continued until RT-QuIC reactivity reached ≤ 1 out of 4 replicates. The seeding dose giving ThT positivity in 50% of replicate wells (SD_{50}) based on the Spearman-Kärber equations was calculated as described [24, 25].

Statistical analysis

The statistical comparisons were performed using t-tests and one-way ANOVA for comparing two or more groups, respectively (GraphPad Prism Software Version 9.0.0). Data were expressed as means \pm SD (standard deviation) or SE (standard error of the mean). A two-sided type I error level of 0.05 was adopted. The statistically significant differences were expressed as * $p < 0.05$, ** $p < 0.01$, *** $p < 0.005$, and **** $p < 0.001$ or $p < 0.0001$, as indicated. The number of biological replicates was expressed as “n”, and 4 technical replicates was used for each biological sample.

Results

Streamlined α Syn RT-QuIC assay

Our streamlined RT-QuIC assay protocol was developed based on the second-generation platform of α Syn RT-QuIC as described by Caughey and colleagues [15], with the following modifications. We acquired all assay reagents from commercial sources, including the monomeric rec-Syn protein, the substrate present in vast excess for in vitro conversion into amyloid fibrils by seeding with minute quantities of α Syn^D aggregates from a clinical sample to be examined. This approach eliminated the need for the laborious and lengthy (~5–7 days) in-house production and purification of rec-Syn by highly specialized personnel, and minimized the variability in the quality of rec-Syn produced [15]. Following a screen of rec-Syn products from several sources, we found that a commercial product of monomeric human wild-type rec-Syn (rPeptide) was most suitable for this RT-QuIC assay (see [Methods](#) section). Two separate lots of the commercial rec-Syn protein were successfully used for the RT-QuIC assay with ~300 reaction plates over a two-year period. Accordingly, our simplified α Syn RT-QuIC assay involved minimal hands-on time (~1 h) to rapidly assemble all reagents for RT-QuIC reactions in a 96-well plate, sufficient for testing 24 samples in quadruplicate. Moreover, we markedly shortened the preanalytical processing of peripheral tissues by eliminating a 4-h enzymatic digestion step used in previous studies [20, 23].

In addition, the ThT concentration was increased from 10 μM to 20 μM to minimize self-quenching of ThT fluorescence [26]. Finally, we found that a single streamlined RT-QuIC assay protocol worked equally well for several different types of tissues including the brain, skin, salivary gland, and colon.

RT-QuIC assay of $\alpha\text{Syn}^{\text{D}}$ seeding activity in brain homogenates of PD and DLB

To verify that our streamlined RT-QuIC assay is able to detect the seeding activity of $\alpha\text{Syn}^{\text{D}}$, we first examined brain homogenate (BH) prepared from neuropathologically confirmed cases of PD ($n=3$), DLB ($n=3$), and from NS controls ($n=3$). The RT-QuIC seeding activity of $\alpha\text{Syn}^{\text{D}}$ aggregates in biospecimens was measured as time-dependent increases in ThT fluorescence intensity above background threshold [14, 15]. As expected, $\alpha\text{Syn}^{\text{D}}$ seeding activity was readily detected using our streamlined RT-QuIC assay. RT-QuIC reactions seeded by 2 μl of BH from cases of PD and DLB serially diluted to 10^{-3} through 10^{-8} showed varying degrees of ThT responses within 60 h (Fig. 1a). In contrast, no seeding activity was observed with BH from NS controls at dilutions of 10^{-3} through 10^{-6} (Fig. 1a). RT-QuIC reactions seeded by BH showed a lag phase ranging from 10 to 50 h, with DLB cases displaying shorter lag phase than PD cases at respective dilutions (Fig. 1b). To better characterize the RT-QuIC kinetics, protein aggregation rate (PAR), defined as the inverse of the lag phase (1/h), was used for measuring the rate of seeding activity at each dilution [27]. A dose-dependent increase in PAR was observed in BH-seeded RT-QuIC reactions from both PD and DLB cases (Fig. 1c). Moreover, PAR was significantly higher in DLB than PD across several orders of magnitudes in BH dilutions (Fig. 1c), consistent with higher levels of $\alpha\text{Syn}^{\text{D}}$ aggregates known to be present in brains of DLB patients as compared to those with PD [28]. Our results are in agreement with those in the published study of the second-generation αSyn RT-QuIC assay using in-house generated rec-Syn preparations [15], with similar RT-QuIC kinetics (within 60 h) at comparable dilutions of BH from PD and DLB. Taken together, these results confirmed the feasibility of using commercially available rec-Syn for an ultrasensitive RT-QuIC assay of $\alpha\text{Syn}^{\text{D}}$ in million-fold diluted BH of PD and DLB.

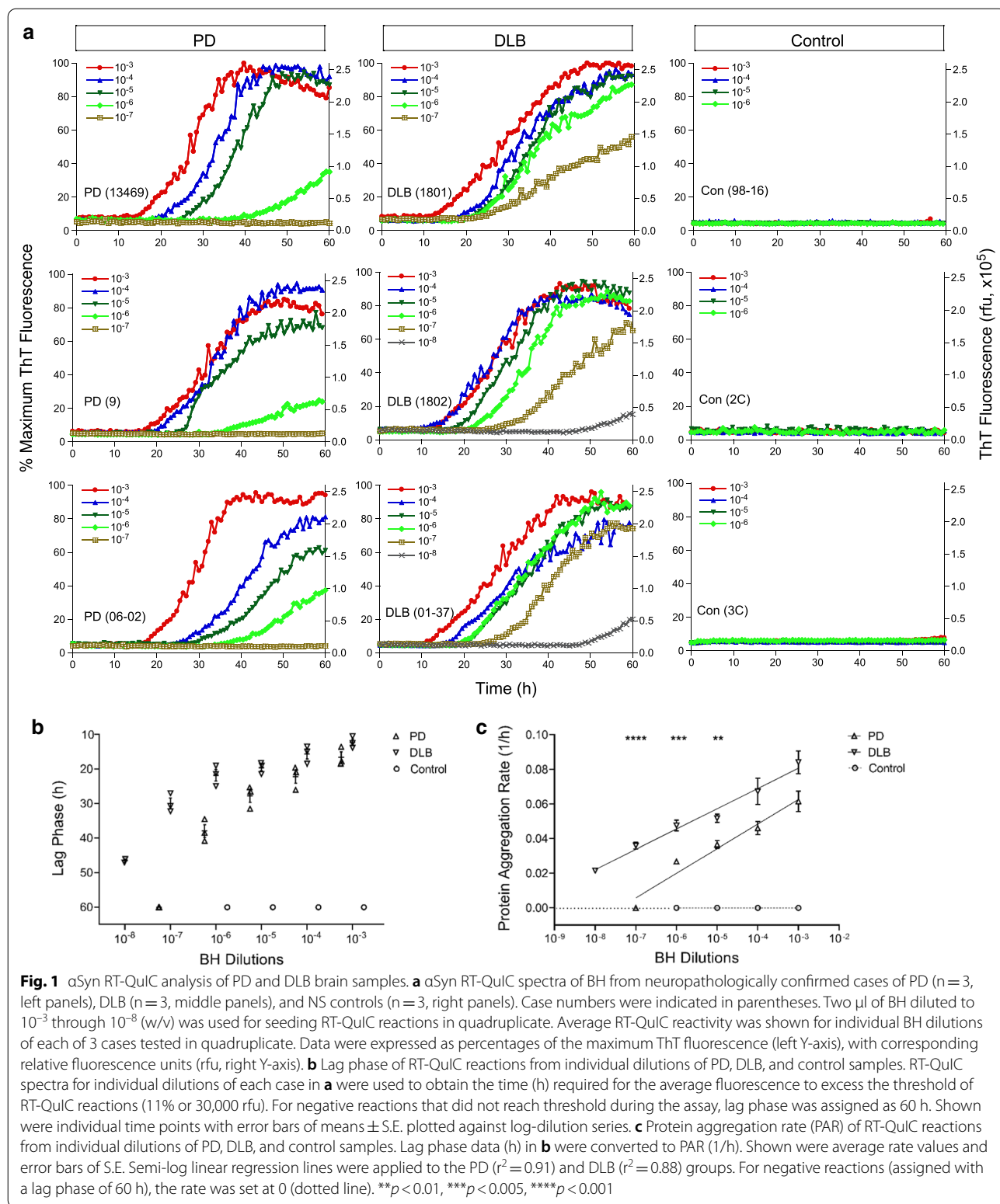
Ultrasensitive detection of $\alpha\text{Syn}^{\text{D}}$ seeding activity in CSF samples of PD and DLB

After we successfully detected $\alpha\text{Syn}^{\text{D}}$ in highly diluted BH of PD and DLB cases, we next evaluated the sensitivity of our RT-QuIC assay for postmortem CSF samples. As reported previously, addition of a small amount of SDS (0.0015%) is necessary to bring the CSF-seeded RT-QuIC

reactions to completion within 60 h [15]. In our protocol, the level of SDS was further reduced to 0.0005% (5 ppm) (see [Methods](#) section). CSF samples were acquired from neuropathologically confirmed cases of PD ($n=4$), DLB ($n=4$), as well as NS controls ($n=2$), and 2 μl of CSF either undiluted or serially diluted to 10^{-1} – 10^{-3} , equivalent to 2–0.002 μl of CSF, respectively, was used to seed RT-QuIC reactions. Seeding activity was detectable in PD and DLB cases but not in controls at all CSF levels, and remarkably, even in as little as 0.002 μl of CSF (Fig. 2a). The lag phase varied from 12 to 45 h in CSF-seeded RT-QuIC reactions, with a shorter lag phase in DLB than PD in RT-QuIC reactions seeded by 0.02–2 μl CSF (Fig. 2b). Accordingly, PAR was significantly higher in DLB than in PD at the respective CSF levels (Fig. 2c). Interestingly, for both PD and DLB, PAR increased when seeding went from 0.002 μl to 0.02 μl of CSF, but plateaued at 0.2 μl CSF and even decreased at 2 μl of undiluted neat CSF (Fig. 2b). Thus, non-linear RT-QuIC responses seemed to occur at higher seeding doses of CSF. This is likely due to the presence of putative inhibitors in undiluted samples that may suppress initial RT-QuIC reactions which subsequently rebound upon dilutions, consistent with the previous observations as reported [29, 30]. In summary, our streamlined RT-QuIC assay enabled ultrasensitive detection of $\alpha\text{Syn}^{\text{D}}$ in PD and DLB cases using only nanoliters of CSF.

Analytical performance of the streamlined RT-QuIC assay for CSF samples of PD and DLB

To further evaluate the diagnostic utility of the streamlined αSyn RT-QuIC assay, we acquired a large number of postmortem CSF samples from neuropathologically confirmed cases of PD, DLB, and NS controls from the NIH NeuroBioBank (NBB), a centralized network of biorepositories. All CSF samples were evaluated at the 0.2 μl seeding level (2 μl of tenfold dilution of neat CSF) for RT-QuIC reactions in quadruplicate with a throughput of 24 samples (including positive and negative controls) in a single 96-well plate per assay. We first examined the RT-QuIC profile in a set of 40 cases of PD and 40 NS controls. CSF samples from PD cases displayed positive RT-QuIC responses within ~18–50 h (Fig. 3a). For comparison, we tested another set of 30 cases each for DLB and NS controls. RT-QuIC of CSF samples from DLB cases exhibited strong ThT responses within ~15–30 h (Fig. 3b). NS controls showed negative reactivity below the threshold within 60 h. The overall RT-QuIC kinetics of CSF samples from PD cases exhibited a slower and broader RT-QuIC reactivity as compared to that of DLB (Fig. 3a vs. Figure 3b), as observed in a previous study of a small cohort of CSF samples from PD and DLB patients



[15], suggesting a differential pattern of RT-QuIC kinetics between CSF samples from PD and DLB patients.

In total, our RT-QuIC assay examined 214 postmortem CSF samples from 88 cases of PD, 58 cases of DLB, and 68 cases of NS controls [neurologically normal ($n=23$), ALS ($n=9$), MS ($n=6$), AD ($n=7$), Pick's disease ($n=10$), CBD ($n=4$), and PSP ($n=9$)]. Analysis of the CSF seeding activity at the end of the 60 h RT-QuIC assay revealed an excellent analytical performance for both PD and DLB (Fig. 3c). Positive seeding activity was observed in 86 out of 88 CSF samples in the PD group and 57 out of 58 CSF samples in the DLB group, yielding a sensitivity of 98% for both PD and DLB. None of the 68 NS control CSF samples showed positive seeding activity, resulting in a specificity of 100%. In comparison, the overall CSF seeding activity was significantly higher in DLB than PD ($p < 0.05$), and the combined PD and DLB group was well above NS controls ($p < 0.0001$). Taken together, these results confirm that CSF is a useful specimen for validating the RT-QuIC assay as a robust tool for the diagnosis of PD and DLB.

Single RT-QuIC assay platform for multiple biospecimens of PD

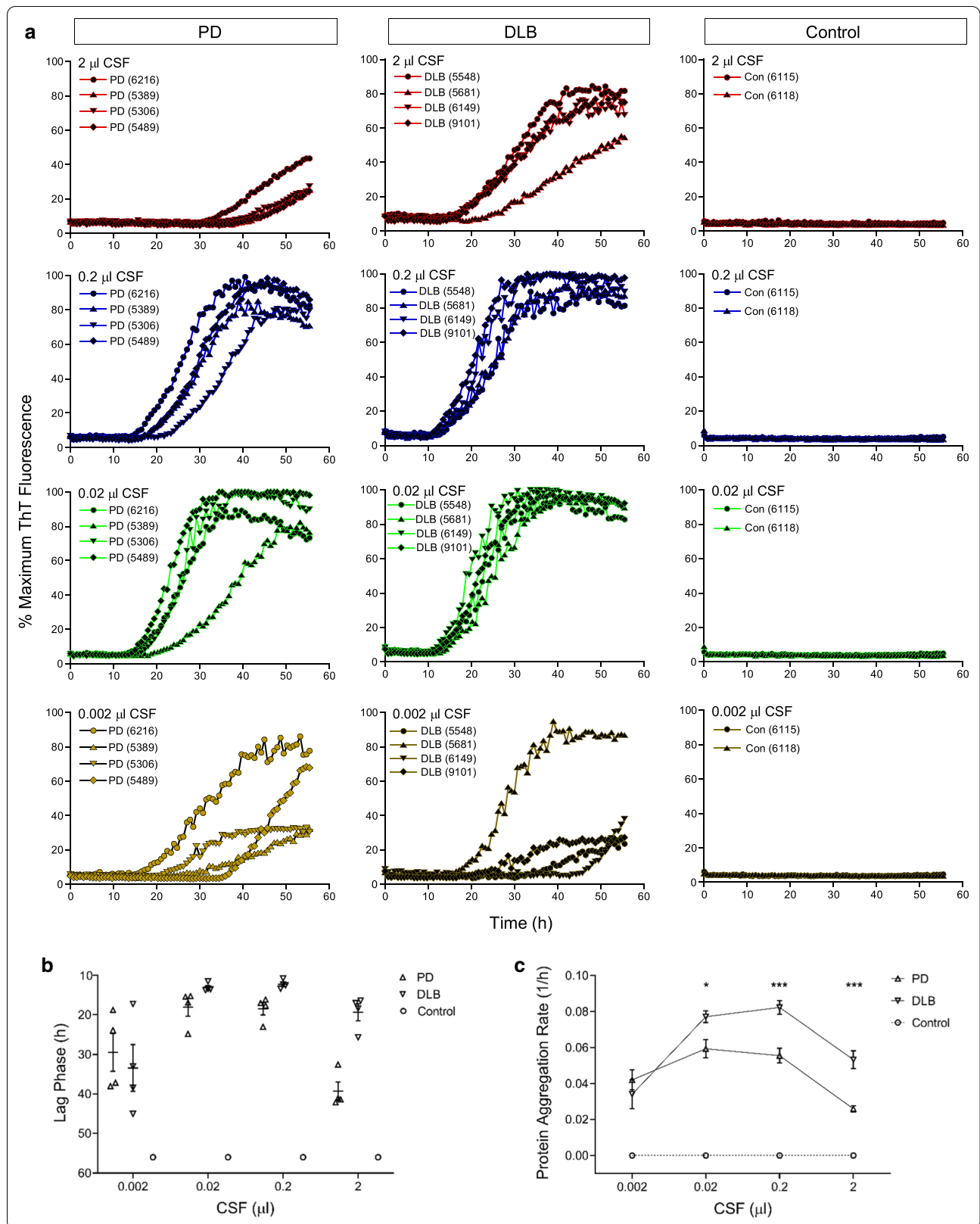
Finally, we examined whether our streamlined RT-QuIC assay can be used for different types of specimens without the need to modify assay conditions. Several types of biospecimens were collected from the same PD cadavers, subjected to the same processing and serial dilution procedure, and tested under the same RT-QuIC assay conditions. Spearman-Kärber endpoint dilution analysis was used to determine the seeding dose at which 50% of replicate reactions were positive, termed SD_{50} [24]. In a neuropathologically confirmed PD case from whom scalp skin was available in addition to the brain and CSF, we performed parallel RT-QuIC reactions seeded with the respective specimens in tenfold dilution series (from 10^{-1} through 10^{-8}). As shown in Fig. 4a, αSyn^D seeding activity displayed dose-dependent titration in serially diluted PD samples of BH, skin homogenate, and CSF, respectively. The Spearman-Kärber analysis of this PD case yielded

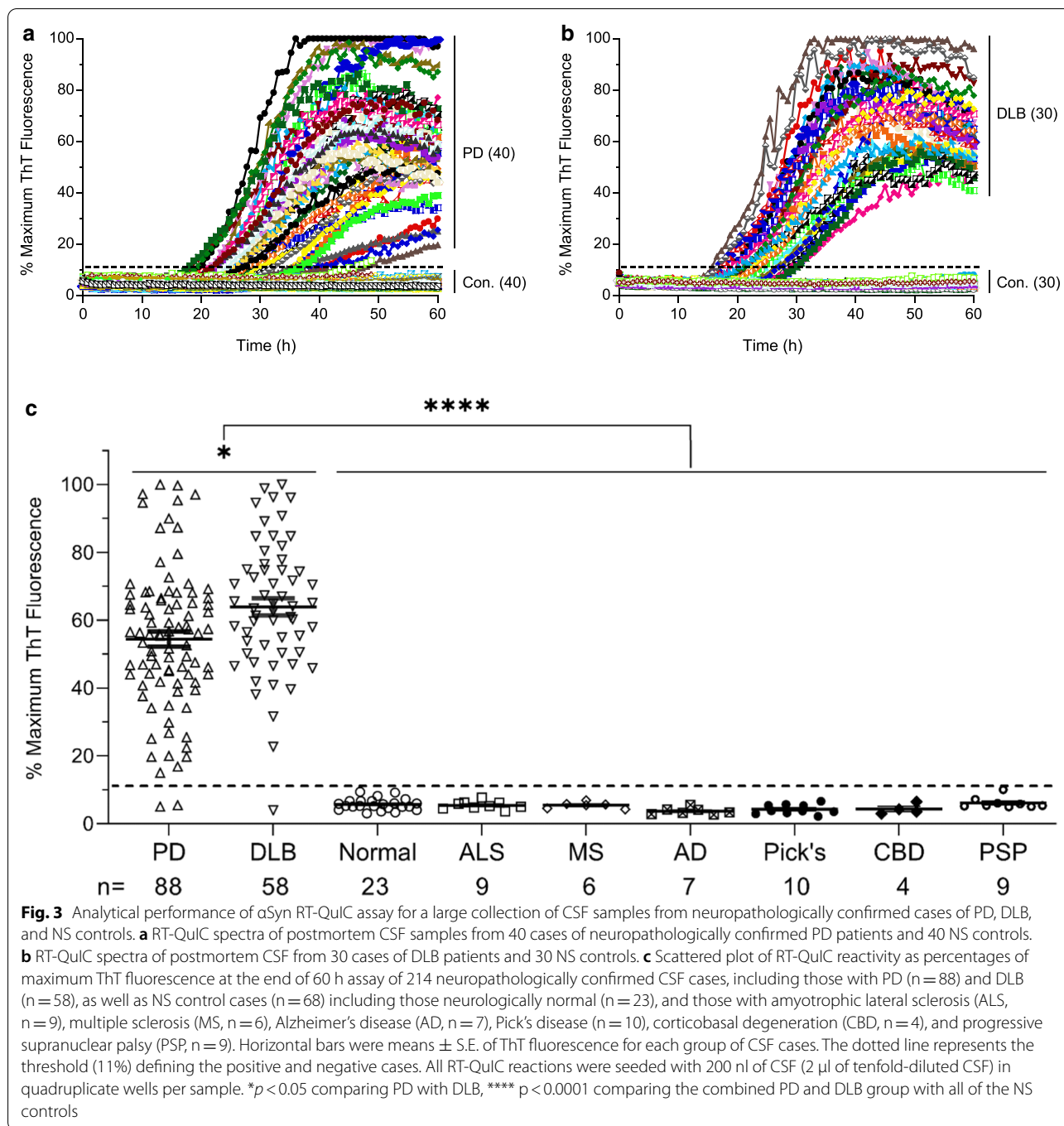
SD_{50} values at $2.8 \times 10^6/\text{mg}$ for the brain, $5.0 \times 10^4/\text{mg}$ for the skin, and $2.8 \times 10^3/\mu\text{l}$ for CSF. No seeding activity was detected in corresponding biospecimens from a control cadaver affected by AD (Fig. 4a). To explore more broadly the tissue distribution of αSyn^D , another case of neuropathologically confirmed PD was examined from which scalp skin, submandibular salivary gland (SMG), and sigmoid colon were available in addition to CSF. Using the same RT-QuIC assay protocol, αSyn^D seeding activity was examined in serially diluted tissue homogenates of skin, SMG, and colon, and in serially diluted CSF (Fig. 4b). SD_{50} values obtained from Spearman-Kärber analysis of this PD case were $5.0 \times 10^4/\text{mg}$ for skin, $8.9 \times 10^5/\text{mg}$ for SMG, $8.9 \times 10^4/\text{mg}$ for colon, and $2.8 \times 10^2/\mu\text{l}$ for CSF. In contrast, no seeding activity was found in corresponding specimens from a neurologically normal control case (Fig. 4b). Therefore, the αSyn^D seeding activity in PD peripheral tissues of the skin, SMG, and colon was relatively high, ranging from $\sim 10^4$ to $\sim 10^5$ per mg of tissues, which was only 1 to 2 orders of magnitude lower than that in the brain ($\sim 10^6/\text{mg}$). The seeding activity in PD CSF was in the range of 10^2 – 10^3 per μl . For brain and CSF, the previously reported SD_{50} values in PD and DLB were in the range of 10^5 – $10^6/\text{mg}$ and 4–54/ μl , respectively [15]. Thus, our streamlined RT-QuIC assay provides a single unified protocol for robust tracking of αSyn^D seeding activity across multiple biospecimens from the same patients affected by PD and other synucleinopathies.

To evaluate the reliability of our streamlined RT-QuIC protocol, we analyzed tissue homogenates from a third case of neuropathologically confirmed PD using different batches of rec-Syn substrate. Distinct patterns of RT-QuIC kinetics from reactions seeded by PD tissue homogenates from the skin, SMG, and colon were consistently reproduced when performed with two different lots of rec-Syn (Fig. 5). In contrast, only negative reactivity was observed in corresponding tissue homogenates from a neurologically normal control case, confirming the specificity of the RT-QuIC reactions (Fig. 5). Therefore, our streamlined RT-QuIC

(See figure on next page.)

Fig. 2 Ultrasensitive αSyn RT-QuIC assay of CSF samples of PD and DLB. **a** αSyn RT-QuIC spectra of postmortem CSF from neuropathologically confirmed cases of PD ($n=4$, left panels), DLB ($n=4$, middle panels), and NS controls ($n=2$, right panels). Case numbers were indicated in parentheses. RT-QuIC reactions were seeded with 2 μl of CSF either undiluted or serially diluted to 10^{-1} through 10^{-3} (v/v), equivalent to 2–0.002 μl of original CSF. Average RT-QuIC reactivity was shown for individual CSF titrations in 4 cases of PD, 4 cases of DLB, and 2 cases of NS controls tested in quadruplicate. Data were expressed as percentages of the maximum ThT fluorescence. **b** Lag phase of RT-QuIC reactions seeded with individual CSF levels in PD, DLB, and control samples. RT-QuIC spectra for individual CSF levels of each case in **a** were used to obtain the time required for the average fluorescence to exceed the threshold of RT-QuIC reactions (11% or 30,000 rfu). Shown were individual time points with error bars of means \pm S.E. plotted against CSF levels. **c** Protein aggregation rate of RT-QuIC reactions seeded with individual CSF levels in PD, DLB, and control samples. Lag phase data (h) in **b** were converted to protein aggregation rate (1/h). Shown were average rate values and error bars of S.E. For negative reactions, the rate was set at 0 (dotted line). * $p < 0.05$, *** $p < 0.005$



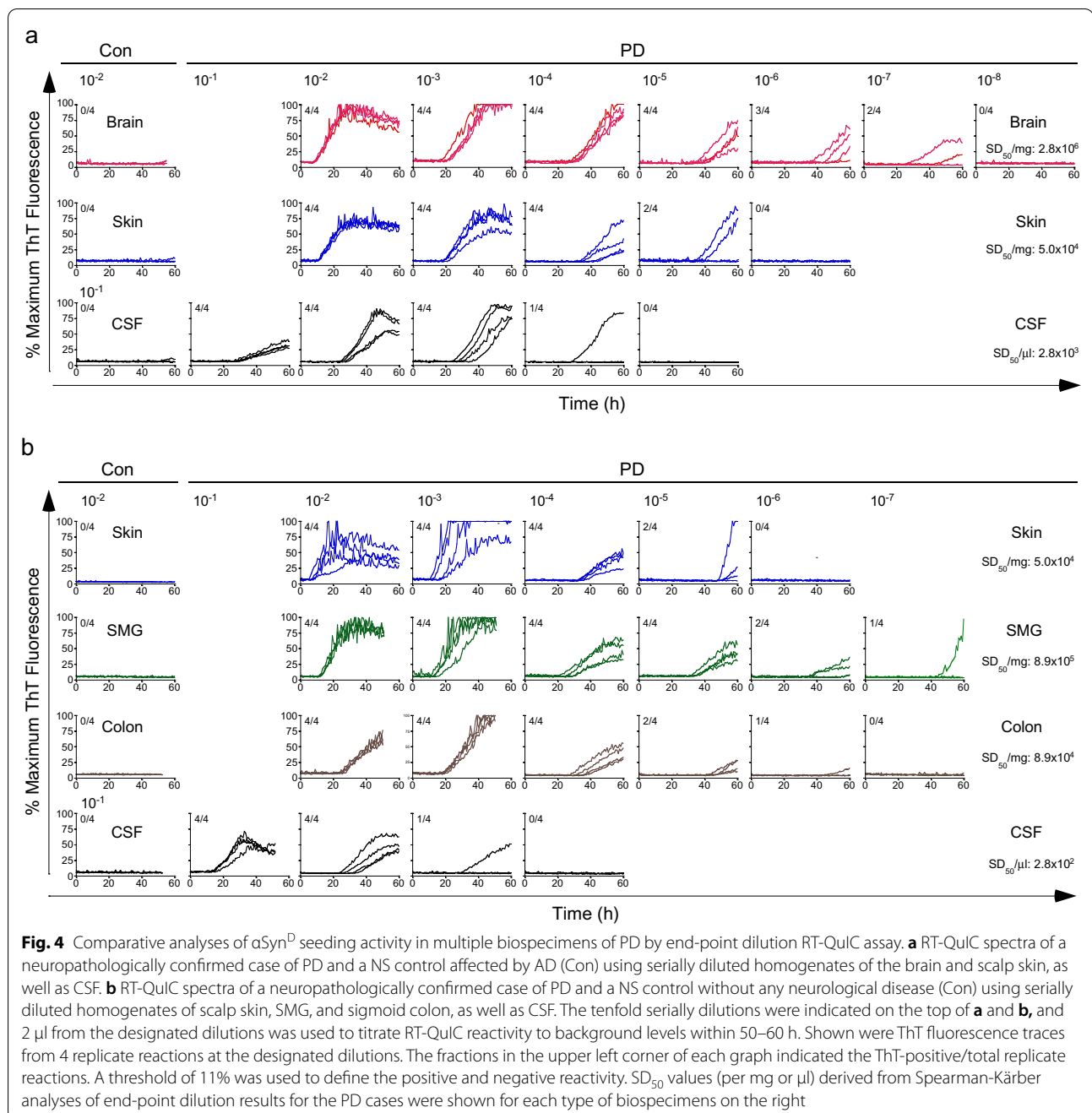


assay enables reliable and robust analysis of α Syn^D seeding activity in various patient-derived specimens.

Discussion

α Syn RT-QuIC has recently gained popularity due to its ability to detect the seeding activity of α Syn^D aggregates in clinical specimens. Initial applications have been

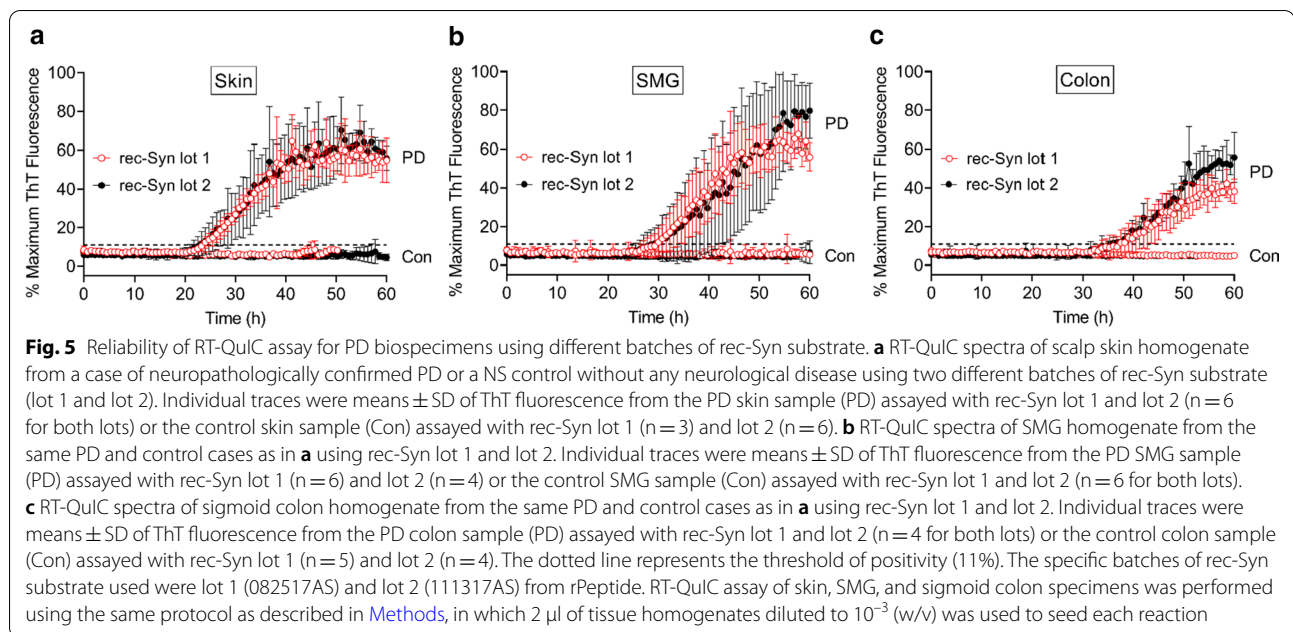
demonstrated by several groups using BH and CSF of PD and DLB. However, existing α Syn RT-QuIC assay protocols vary in configuration, length of assay, tissue processing, as well as the compositions and sources of reagents [14–17, 31]. We have now developed a streamlined α Syn RT-QuIC assay for various biospecimens of PD and DLB, with optimized reagent compositions and a single tissue extraction procedure, resulting in a



simplified and improved assay platform that can be easily implemented in a routine laboratory.

A key reagent for the α Syn RT-QuIC assay is rec-Syn that serves as the substrate for seeded fibrillization. In many published studies, rec-Syn is produced in-house, which often introduces batch-to-batch variability and requires considerable expertise and personnel to ensure the production of high quality rec-Syn protein during prolonged in-house preparation and purification steps

(~5–7 days). We have developed a streamlined α Syn RT-QuIC assay based on the second-generation platform [15] and opted for entirely commercial reagents including rec-Syn in an effort to simplify and standardize the assay conditions. As a result, our streamlined α Syn RT-QuIC assay requires a single technician with a hands-on time of ~1 h to set up 96-reaction wells in a multi-well plate for unattended readouts from a plate reader. Therefore, our simplified protocol drastically lessens the technical barrier to



the implementation of the highly efficient α Syn RT-QuIC assay in a routine laboratory. An upward adjustment of ThT concentrations (from 10 μ M to 20 μ M) was also incorporated to offset the self-quenching of ThT fluorescence upon binding to amyloid fibrils as reported in a previous study [26].

We have extensively tested our streamlined α Syn RT-QuIC protocol against neuropathologically confirmed cases of PD and DLB using BH and CSF. To validate its diagnostic value for PD and DLB, we performed α Syn RT-QuIC analysis of a large panel of 214 CSF samples, yielding an overall sensitivity of 98% and a specificity of 100%. Our results are consistent with other reports of overall high diagnostic accuracy of α Syn RT-QuIC analyses of CSF from various PD and DLB cohorts from different populations [14–17, 31]. Therefore, it is foreseeable that a standardized RT-QuIC assay of CSF will offer added diagnostic values for both PD and DLB. Notably, we observed α Syn^D seeding activity in a much lower sample volume (0.02–0.2 μ l) of ventricular CSF obtained at autopsy than that required for premortem lumbar CSF (15–20 μ l) [14–17, 31]. This discrepancy could be due to higher levels of α Syn^D in autopsy CSF than those in premortem patients. Alternatively, the assay sensitivity could be influenced by a difference in biochemical and cytological compositions between ventricular and lumbar CSF [32], including a difference in the levels of salts [33] since some inorganic ions have been found to modulate the performance of RT-QuIC in different sample matrices [34]. Nonetheless, our findings have confirmed the value of archived CSF from well-characterized cases as a

reference material for RT-QuIC assay development and validation.

Previous studies using IHC staining have observed abnormally phosphorylated α Syn in non-CNS organs of PD and DLB patients [9–11, 35–38]. However, technical challenges of the IHC-based method may have limited its clinical utility [39]. Most recently, several tissue-specific α Syn RT-QuIC platforms have been reported with nasal brushing [18], SMG [19] and skin [20, 21] samples from PD patients, but procedures for tissue extraction and reagent compositions for RT-QuIC assay differed for individual tissues and among different studies. Therefore, a simplified and standardized protocol is desired to uniformly perform RT-QuIC assay and compare distribution of α Syn^D among multiple tissue types. In our assay protocol, we extracted all tissues with bead-based homogenization in the same buffer, eliminated an enzymatic digestion step lasting for 4 h, and performed RT-QuIC assay under identical conditions. Thus, we have provided a single and simplified RT-QuIC protocol for concurrent detection of α Syn^D in different tissues. Using Spearman-Kärber analysis of endpoint dilution experiments, we have demonstrated the utility of our RT-QuIC assay for a parallel and quantitative comparison of α Syn^D seeding activity (in SD_{50} units) for multiple PD specimens including the skin, SMG, colon, and CSF, all of which are clinically accessible. In short, our RT-QuIC assay protocol supports the measurement of α Syn^D seeding activity in different biospecimens under the same assay conditions.

Our RT-QuIC assay has enabled ultrasensitive detection of α Syn^D seeding activity in highly diluted specimens

of PD and DLB, up to million-fold dilution for BH and several thousand-fold dilution for peripheral tissues, and in nanoliters of CSF. Given the high costs of patient recruitment and specimen procurement, the extremely low sample consumption afforded by our RT-QuIC assay will facilitate the efficient use and sharing of scarce resources of biospecimens collected during various clinical studies. As a reliable and robust tool, the ultrasensitive RT-QuIC assay platform has several attributes that will allow for easy translation into the clinical arena, including rapid turnaround, high throughput, and ultrasensitive and automated readouts. Indeed, the prion RT-QuIC assay of CSF has been incorporated into the updated diagnostic criteria for Creutzfeldt-Jakob disease since 2018 [40]. Future efforts to incorporate the α Syn RT-QuIC assay into clinical practice will require analytical and clinical validation using large collections of pre-mortem patient samples at multiple sites. It is plausible that a standardized and clinically validated α Syn RT-QuIC assay for clinically accessible biospecimens, including CSF and various peripheral tissues, will serve as a diagnostic biomarker of PD and DLB.

Conclusions

In summary, we have developed a streamlined RT-QuIC assay platform for ultrasensitive detection of α Syn^D in a diverse array of biospecimens from postmortem PD and DLB patients. The streamlined protocol requires minimal hands-on time and technical expertise to set up the RT-QuIC assay. This optimized platform could facilitate easy implementation of this α Syn RT-QuIC assay in a routine laboratory, and enable the standardization of the assay across different sites. We have verified the analytical sensitivity and specificity of a streamlined RT-QuIC assay in a large number of postmortem CSF samples of PD and DLB cases. Moreover, we have demonstrated that a single RT-QuIC protocol is suitable to detect α Syn^D seeding activity in multiple tissue specimens such as the brain, skin, salivary gland, and colon. Finally, our assay is ultrasensitive, high-throughput, low on sample consumption, and easy to adapt to different biospecimens. The ongoing evaluation of α Syn^D as a potential biomarker of PD and DLB in clinically accessible biospecimens has broad implications for understanding disease pathogenesis, improving clinical and differential diagnosis, and monitoring efficacy of treatments and neuroprotective agents in clinical trials.

Acknowledgements

We are indebted to the NIH NeuroBioBank for providing many cases of human brain, skin, and CSF samples used in this study, the University of Maryland Brain and Tissue Bank for selection of brain, skin, and CSF cases, and the brain bank at Icahn School of Medicine at Mount Sinai for selection of CSF cases of DLB. We are grateful to the Banner Sun Health Research Institute Brain and

Body Donation Program of Sun City, Arizona (directed by Dr. Thomas Beach) for the provision of some autopsy samples of CSF, skin, SMG, and sigmoid colon.

Authors' contributions

SGC designed the study. SGC and JM supervised and coordinated the data analysis. CB and SGC wrote the manuscript. CB and WW performed RT-QuIC experiments. SAG provided clinical expertise. SAG, AJL, NS, BA, ZW, and WZ provided CSF samples for pilot experiments. XZ, RX, WZ reviewed experimental data. CT helped statistical analyses. VH provided clinical expertise and coordinated the tissue procurement from Mount Sinai brain bank. AL coordinated the tissue procurement from University of Maryland Brain and Tissue Bank. SAG, RX, WZ, and SGC obtained funding support. All authors read and approved the final version of manuscript.

Funding

This study was supported in part by the American Parkinson Disease Association (to SGC), the US National Institutes of Health (NIH)/National Institute on Aging (R01AG061388 to RX and SGC), and NIH/National Institute of Neurological Disorders and Stroke (U01NS112010 to WZ, SAG, and SGC, and R01NS118760 to SGC). The funders of the study had no role in the study design, data collection, analysis, and interpretation, or the decision to submit for publication.

Availability of data and materials

All data are available upon reasonable request to the corresponding authors.

Declarations

Ethics approval and consent to participate

The procurement and use of archived human tissues were authorized by the institutional review boards at Case Western Reserve University and individual biorepositories, and by relevant material transfer agreements. All specimens and associated clinical data were received in a coded and de-identified manner according to NIH guidelines and HIPAA regulations.

Consent for publication

Not applicable.

Competing interests

The authors declare that they have no competing interests.

Author details

¹ Department of Pathology, Case Western Reserve University School of Medicine, Cleveland, OH 44106, USA. ² Department of Neurology, University Hospitals Cleveland Medical Center, Case Western Reserve University School of Medicine, Cleveland, OH 44106, USA. ³ University of Maryland Brain and Tissue Bank, Baltimore, MD 21201, USA. ⁴ Department of Population and Quantitative Health Sciences, Case Western Reserve University School of Medicine, Cleveland, OH 44106, USA. ⁵ Department of Psychiatry, Icahn School of Medicine at Mount Sinai, New York, NY 10029, USA. ⁶ Van Andel Institute, Grand Rapids, MI 49503, USA.

Received: 28 February 2021 Accepted: 31 March 2021

Published online: 07 April 2021

References

- Chen-Plotkin AS, Albin R, Alcalay R, Babcock D, Bajaj V, Bowman D et al (2018) Finding useful biomarkers for Parkinson's disease. *Science Transl Med* 10:eaam6003.
- Braak H, Del Tredici K, Rub U, de Vos RA, Jansen Steur EN, Braak E (2003) Staging of brain pathology related to sporadic Parkinson's disease. *Neurobiol Aging* 24:197–211
- Outeiro TF, Koss DJ, Erskine D, Walker L, Kurzawa-Akanbi M, Burn D et al (2019) Dementia with Lewy bodies: an update and outlook. *Mol Neurodegener* 14:5

4. Henderson MX, Trojanowski JQ, Lee VM (2019) α -Synuclein pathology in Parkinson's disease and related α -synucleinopathies. *Neurosci Lett* 709:1343–1346
5. Kalia LV (2019) Diagnostic biomarkers for Parkinson's disease: focus on α -synuclein in cerebrospinal fluid. *Parkinsonism Relat Disord* 59:21–25
6. Eusebi P, Giannandrea D, Biscetti L, Abraha I, Chiasserini D, Orso M et al (2017) Diagnostic utility of cerebrospinal fluid alpha-synuclein in Parkinson's disease: A systematic review and meta-analysis. *Mov Disord* 32:1389–1400
7. Mollenhauer B, Parnetti L, Rektorova I, Kramberger MG, Pikkarainen M, Schulz-Schaeffer WJ et al (2016) Biological confounders for the values of cerebrospinal fluid proteins in Parkinson's disease and related disorders. *J Neurochem* 139(Suppl 1):290–317
8. Miki Y, Tomiyama M, Ueno T, Haga R, Nishijima H, Suzuki C et al (2010) Clinical availability of skin biopsy in the diagnosis of Parkinson's disease. *Neurosci Lett* 469:357–359
9. Donadio V, Incensi A, Leta V, Giannoccaro MP, Scaglione C, Martinelli P et al (2014) Skin nerve alpha-synuclein deposits: a biomarker for idiopathic Parkinson disease. *Neurology* 82:1362–1369
10. Donadio V, Incensi A, Rizzo G, Capellari S, Pantieri R, Stanzani Maserati M et al (2017) A new potential biomarker for dementia with Lewy bodies: Skin nerve alpha-synuclein deposits. *Neurology* 89:318–326
11. Doppler K, Ebert S, Uceyler N, Trenkwalder C, Ebentheuer J, Volkman J et al (2014) Cutaneous neuropathy in Parkinson's disease: a window into brain pathology. *Acta Neuropathol* 128:99–109
12. Gelpi E, Navarro-Otano J, Tolosa E, Gaig C, Compta Y, Rey MJ et al (2014) Multiple organ involvement by alpha-synuclein pathology in Lewy body disorders. *Mov Disord* 29:1010–1018
13. Saijo E, Groveman BR, Kraus A, Metrick M, Orru CD, Hughson AG et al (2019) Ultrasensitive RT-QuIC seed amplification assays for disease-associated tau, alpha-synuclein, and prion aggregates. *Methods Mol Biol* 1873:19–37
14. Fairfoul G, McGuire LI, Pal S, Ironside JW, Neumann J, Christie S et al (2016) Alpha-synuclein RT-QuIC in the CSF of patients with alpha-synucleinopathies. *Annals Clin Transl Neurol* 3:812–818
15. Groveman BR, Orru CD, Hughson AG, Raymond LD, Zanusso G, Ghetti B et al (2018) Rapid and ultra-sensitive quantitation of disease-associated alpha-synuclein seeds in brain and cerebrospinal fluid by alphaSyn RT-QuIC. *Acta Neuropathol Commun* 6:7
16. Kang UJ, Boehme AK, Fairfoul G, Shah Nawaz M, Ma TC, Hutten SJ et al (2019) Comparative study of cerebrospinal fluid alpha-synuclein seeding aggregation assays for diagnosis of Parkinson's disease. *Mov Disord* 34:536–544
17. Bongianini M, Ladogana A, Capaldi S, Klotz S, Baiardi S, Cagnin A et al (2019) alpha-Synuclein RT-QuIC assay in cerebrospinal fluid of patients with dementia with Lewy bodies. *Annals Clin Transl Neurol* 6:2120–2126
18. De Luca CMG, Elia AE, Portaleone SM, Cazzaniga FA, Rossi M, Bistaffa E et al (2019) Efficient RT-QuIC seeding activity for alpha-synuclein in olfactory mucosa samples of patients with Parkinson's disease and multiple system atrophy. *Transl Neurodegener* 8:24
19. Manne S, Kondru N, Jin H, Anantharam V, Huang X, Kanthasamy A et al (2020) Alpha-synuclein real-time quaking-induced conversion in the submandibular glands of Parkinson's disease patients. *Mov Disord* 35:268–278
20. Wang Z, Becker K, Donadio V, Siedlak S, Yuan J, Rezaee M et al (2021) Skin alpha-synuclein aggregation seeding activity as a novel biomarker for Parkinson disease. *JAMA Neurol* 78:30–40
21. Manne S, Kondru N, Jin H, Serrano GE, Anantharam V, Kanthasamy A et al (2020) Blinded RT-QuIC analysis of alpha-synuclein biomarker in skin tissue from Parkinson's disease patients. *Mov Disord* 35:2230–2239
22. Manne S, Kondru N, Hepker M, Jin H, Anantharam V, Lewis M et al (2019) Ultrasensitive detection of aggregated alpha-synuclein in glial cells, human cerebrospinal fluid, and brain tissue using the RT-QuIC assay: new high-throughput neuroimmune biomarker assay for Parkinsonian disorders. *J Neuroimmune Pharmacol* 14:423–435
23. Orru CD, Yuan J, Appleby BS, Li B, Li Y, Winner D et al (2017) Prion seeding activity and infectivity in skin samples from patients with sporadic Creutzfeldt-Jakob disease. *Sci Transl Med* 9:eaaam7785.
24. Wilham JM, Orru CD, Bessen RA, Atarashi R, Sano K, Race B et al (2010) Rapid end-point quantitation of prion seeding activity with sensitivity comparable to bioassays. *PLoS Pathog* 6:e1001217
25. Dougherty RM (1964) Animal virus titration techniques. In: Harris RJC (ed) *Techniques in experimental virology*. Academic Press, New York, pp 183–186
26. Lindberg DJ, Wenger A, Sundin E, Wesen E, Westerlund F, Esbjorner EK (2017) Binding of thioflavin-T to amyloid fibrils leads to fluorescence self-quenching and fibril compaction. *Biochemistry* 56:2170–2174
27. Hoover CE, Davenport KA, Henderson DM, Pulscher LA, Mathiason CK, Zabel MD et al (2016) Detection and quantification of CWD prions in fixed paraffin embedded tissues by real-time quaking-induced conversion. *Sci Rep* 6:25098
28. Adamowicz DH, Roy S, Salmon DP, Galasko DR, Hansen LA, Masliah E et al (2017) Hippocampal alpha-synuclein in dementia with Lewy bodies contributes to memory impairment and is consistent with spread of pathology. *J Neurosci* 37:1675–1684
29. Cramm M, Schmitz M, Karch A, Mitrova E, Kuhn F, Schroeder B et al (2016) Stability and reproducibility underscore utility of RT-QuIC for diagnosis of Creutzfeldt-Jakob disease. *Mol Neurobiol* 53:1896–1904
30. Davenport KA, Hoover CE, Denkers ND, Mathiason CK, Hoover EA (2018) Modified protein misfolding cyclic amplification overcomes real-time quaking-induced conversion assay inhibitors in deer saliva to detect chronic wasting disease prions. *J Clin Microbiol* 56:e00947-e1018
31. Rossi M, Candelise N, Baiardi S, Capellari S, Giannini G, Orru CD et al (2020) Ultrasensitive RT-QuIC assay with high sensitivity and specificity for Lewy body-associated synucleinopathies. *Acta Neuropathol* 140:49–62
32. Torres-Corzo JG, Tapia-Pérez JH, Sánchez-Aguilar M, Della Vecchia RR, Chalita Williams JC, Cerda-Gutiérrez R (2009) Comparison of cerebrospinal fluid obtained by ventricular endoscopy and by lumbar puncture in patients with hydrocephalus secondary to neurocysticercosis. *Surg Neurol* 71:376–379
33. Garland J, Philcox W, Kesha K, Morrow P, Lam L, Spark A et al (2018) Differences in sampling site on postmortem cerebrospinal fluid biochemistry: a preliminary study. *Am J Forensic Med Pathol* 39:304–308
34. Metrick MA 2nd, do Carmo Ferreira N, Saijo E, Hughson AG, Kraus A, Orru C, et al (2019) Million-fold sensitivity enhancement in proteopathic seed amplification assays for biospecimens by Hofmeister ion comparisons. *Proc Natl Acad Sci USA* 116:23029–23039
35. Braak H, de Vos RA, Bohl J, Del Tredici K (2006) Gastric alpha-synuclein immunoreactive inclusions in Meissner's and Auerbach's plexuses in cases staged for Parkinson's disease-related brain pathology. *Neurosci Lett* 396:67–72
36. Beach TG, Adler CH, Sue LI, Vedders L, Lue L, White III CL et al (2010) Multi-organ distribution of phosphorylated alpha-synuclein histopathology in subjects with Lewy body disorders. *Acta Neuropathol* 119:689–702
37. Gibbons CH, Garcia J, Wang N, Shih LC, Freeman R (2016) The diagnostic discrimination of cutaneous alpha-synuclein deposition in Parkinson disease. *Neurology* 87:505–512
38. Zange L, Noack C, Hahn K, Stenzel W, Lipp A (2015) Phosphorylated alpha-synuclein in skin nerve fibres differentiates Parkinson's disease from multiple system atrophy. *Brain* 138:2310–2321
39. Visanji NP, Mollenhauer B, Beach TG, Adler CH, Coffey CS, Kopil CM et al (2017) The Systemic Synuclein Sampling Study: toward a biomarker for Parkinson's disease. *Biomark Med* 11:359–368
40. Rhoads DD, Wrona A, Foutz A, Blevins J, Glisic K, Person M et al (2020) Diagnosis of prion diseases by RT-QuIC results in improved surveillance. *Neurology* 95:e1017–e1026

Publisher's Note

Springer Nature remains neutral with regard to jurisdictional claims in published maps and institutional affiliations.